PEG-FREE HUMAN HAND SHAPE ANALYSIS AND RECOGNITION

Wei Xiong, Changsheng Xu

Institute for Infocomm Research,
21 Heng Mui Keng Terrace,
Singapore 119613

Sim Heng Ong

National University of Singapore,
Department of Electrical & Computer Engineering,
Singapore 117576

ABSTRACT

This work addresses the problem of deformable hand shape recognition in biometric systems without positioning aids. We separate and recognize multiple rigid fingers. An elliptical model is introduced to represent fingers and accelerate the matching of them. Technically, our method bridges the traditional handcrafted-feature methods and the shape-distance methods. We have tested it using our 108-person-540-sample database with significantly increased positive recognition accuracy.

1. INTRODUCTION

After the September-11 event, automatic identification of human becomes more and more important. The hand shape-based authentication technology measures the geometrical shapes of hands and has been widely applied to many areas from home door access controls to nuclear facility protections. The major architectures of these systems and algorithms are almost the same and can be summarized here [1, 2]: 1)A platen is used to support the tested hand and a low/medium-cost and low-resolution CCD camera is used to capture the hand images; 2)Positioning aids such as pegs are used to facilitate the location of hands and fingers and the extraction of features; 3) Up to tens of geometry features including lengths and widths of fingers, aspect ratios of the palm or fingers, the thickness of the hand, the finger perimeter and areas etc. are used; 4) The features of a hand are measured separately utilizing the position information of pegs without referring to other hands.

In most of current works, the geometry features were extracted with reference to the positions of the fixed pegs or other prior position information. Since the hand was assumed to be aligned to the pegs, it was assumed to be aligned with other hands to be compared with as well. There was no search procedure involved for the optimal alignment of hands. As such, the examined hand was required to be placed on the exactly same position in both the enrollment stage and the verification stage. The ill-rigidness of the shape of our hands and fingers introduces variance into the geometry features used for recognition. Thus these *hand-crafted features* obtained in the above manner are neither stable nor reliable [3].

The hand biometric systems using position-fixed pegs may not be suitable for all possible dimensions of hands[1]. We developed a peg-free hand-shape recognition system [4], which is similar to those presented in [2] except for no pegs introduced. To use it, users are advised to put their hands on a flat supporting surface with their fingers separated and stretched naturally. The top-view grey-scale image (see Fig. 1(a) for an example) is captured by a CCD camera and transferred into a PC for processing. The removal of the positioning aids causes two problems. Firstly, the shapes of hands become more deformable. Secondly, the references for locating fingers during hand/finger detection/localization and for geometric feature measurement are also lost. However, we do observe that most parts of the finger away from the root of the finger (except for that of the thumb[2]) are still rigid in normal cases. Hence, we separate every rigid finger and then recognize them. We model each finger as an ellipse with an associated orientation. This provides us a good initialization of the search for optimal finger alignments.

2. METHODOLOGY

The captured hand images are firstly processed. Each of them is thresholded and segmented. The resulted binary image is labelled. The largest labelled object is considered as the hand part, which is reasonable since the region of the imaging system is under control. A boundary following algorithm is applied to trace the hand contour using a set of ordered point sequence. The traced contour of the hand shown in Fig. 1(a) is presented in Fig. 1(b). Next we will analyze the contour and recognize it. Our method includes the following steps: 1) localization of fingertips and valleys; 2) finger identification and separation; 3) finger shape modelling; and 4) finger matching with the help of the models.

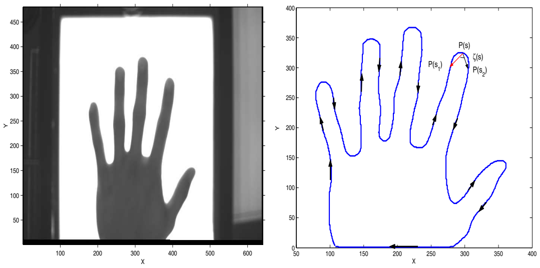

(a) (b)

Fig. 1. (a) A hand image captured; and (b) the traced contour of the detected hand. $P(s)$, $P(s_1)$ and $P(s_2)$ are used to compute $\zeta(s)$ at $P(s)$. Sub pictures plotted here are not in scale.

2.1. Detection and localization of fingertips and valleys

The determined hand contour ϕ is an ordered planar curve in the xy-plane, parameterized by its arc length s. As shown in Fig. 1(b), $P(s)$ or $P = (x, y)$ is any point on it, $\zeta(s)$ is the angle between two vectors $\overrightarrow{PP_1}$ and $\overrightarrow{PP_2}$ taken in the neighborhood of $P(s)$ with $P_1 = P(s_1)$, $P_2 = P(s_2)$ subject to $\Delta s = s - s_1 = s_2 - s$. $\zeta(s)$ is utilized to analyze curvature and to detect corners.

We take $\Delta s = 10$ pixels, which is quite small compared with 3400 pixels, the average hand contour arc length in our database. To avoid missing dominant points, a relatively large threshold (thus a smaller curvature threshold) is applied to threshold $\zeta(s)$. Any contour point whose $\zeta(s)$ is smaller than this threshold will be considered as a *corner*. These *corners* are distributed around the true corners which correspond to fingertips, valleys, and the palm corners far from fingertips. A clustering algorithm is then utilized to separate the clusters. The cluster centers are considered as the true corners. Since these clusters are separated along the contour, we define the distance d between two contour points $P(s_1)$ and $P(s_2)$ along the contour as

$$d = \min(\mathrm{mod}(s_1 - s_2, p), \mathrm{mod}(s_2 - s_1, p)), \qquad (1)$$

where p is the contour arc length and $\mathrm{mod}(s, p)$ is the modulus of s modulo p. Besides, the clusters are also separated each other over their Euclidean distance in the xy-plane. Therefore, d and their Euclidean distance are inputs to the clustering algorithm to isolate clusters and corners.

To classify these corners into fingertips, valleys and palm corners, draw a few circles centered at the hand centroid first. The circles have crossover points with the hand contour. Most of them are near the fingers. With this information, the two palm corners can be found. Secondly, the two corners adjacent to the palm corners are fingertips, either that of the thumb or that of the little finger. Thirdly, among the remaining corners, fingertips and valleys interlace each other. Fourthly, if we draw two equal lines by linking one of the true corners (except for the two palm corners) with two other points on the contour to form a triangle, the centroid of the triangle, for a normal hand, is more likely within that finger if the vertex is a fingertip, or within the background if the vertex is a finger valley. Obviously, the length of the equal lines should be appropriately long. Due to this reason, we employ a multiscale method to differentiate fingertips and valleys. We choose three scales, i.e., $1/2$, $1/4$ and $1/8$ of the finger length as the equal-line length and form three triangles for each true corner. The centroid of each triangle is computed. If two of them are within a finger, then this corner is considered as a fingertip otherwise it will be a valley. In Fig. 2(a) the identified corners are shown where fingertips are marked by x markers (denoted by T^m), valleys by circles and palm corners by triangles (denoted by V^n). Here m and n are the orders of fingers and valleys and need to be identified further.

2.2. Finger identification and separation

Having differentiated types of fingertips and valleys, we can separate them out and identify them. First we identify each fingertip and each valley, i.e., determine m and n mentioned above. Through observations, we find that for a normal hand, the difference between the two side lengths of the index finger is the largest among the index, the middle and the ring finger. Hence, by comparing the finger side length differences, the index finger can be identified. In addition, for a left hand index finger, its left side is longer whereas for a right hand index finger, its right side is longer. With this information, we can judge the hand type. Finally, according to the finger orders, all fingertips and valleys can be identified. They are illustrated in Fig. 2(a), where $\Gamma^j = \Gamma^j(x, y)$, $j = 1, 2, \ldots, 5$, denotes for the thumb, the index, the middle, the ring and the little finger respectively, and T^j, $j = 1, 2, \ldots, 5$, for their tips accordingly. The finger valley between the Γ^j and Γ^{j+1} is denoted as V^j, $j = 1, 2, 3, 4$.

We separate each finger using a coarse-to-fine procedure. In the coarse level, a finger is roughly cut off at the two valleys around it. One of them is treated as the reference valley V_r^j,$j = 1, \ldots, 5$, provided that it is associated with the shorter finger side length. Here, V^1, V^2, V^2 (not V^3), V^4 and V^5 are chosen as the reference valleys for finger Γ^1, Γ^2,Γ^3,Γ^4 and Γ^5, respectively. For each finger Γ^j, $j = 1, \ldots, 5$, a point V_a^j is found on the hand contour on the opposite side to V_r^j of Γ^j subject to $|\overrightarrow{T^j V_r^j}| = |\overrightarrow{T^j V_a^j}|$. The partitioned contour between V_r^j and V_a^j and passing T_j is the coarse estimation of the open contour of that finger Γ^j. The cut finger contour and the line which connects V_r^j and V_a^j form ϕ_a^j, the boundary of Γ^j. As an example, Fig.

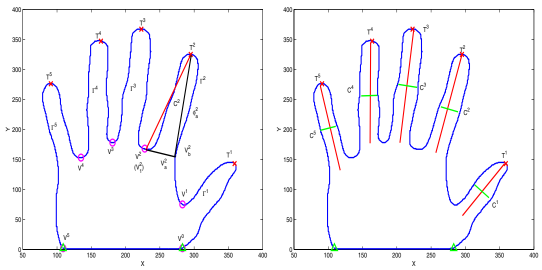

(a) (b)

Fig. 2. (a)The detected fingertips (denoted by x-markers) and valleys (circle markers). (b)The estimated major axis (the longer one within the finger) and the minor axis (the shorter one crossing the finger) of each finger of the hand shape in Fig. 1(b).

2(a) shows V_a^2 and V_b^2 and marks the clipped index finger contour with ϕ_a^2.

In the fine level, V_a^j will be refined. Given Γ^j, the line passing its tip T^j and its refined centroid C^j, defines a reference axis $\overrightarrow{T^jC^j}$. Different from V_r^j, the intersection point V_b^j is found where the hand contour intersects the line passing V_r^j and perpendicular to $\overrightarrow{T^jC^j}$. Passing T^j, the hand contour between V_b^j and V_r^j, and the line segment $V_r^jV_b^j$ form a close contour ϕ^j of the finger Γ^j. From now on Γ^j will refer to the region confined by ϕ^j, i.e., $\Gamma^j = \Gamma^j(x, y)$, $j = 1, \ldots, 5$. To this end, all fingers have been separated and identified.

2.3. Finger shape modelling and hand shape matching

We model a finger as a rigid ellipse which is the best-fitting ellipse of the finger region $\Gamma^j = \Gamma^j(x, y)$ (instead of its boundary ϕ^j only). For Γ^j, linking its center and its fingertip $T^j(x_t^j, y_t^j)$, its major axis is formed orientated at β^j with length L^j. For simplicity, the superscript j indicating which finger shall be omitted in the following if there is no ambiguity. The parameters set of the elliptical model for the j-th finger is represented as

$$\lambda^j = (\beta^j, T^j, L^j, W^j, C^j), \forall j, \tag{2}$$

where L^j and W^j are the lengths of the major and minor axes respectively and $C(x_c, y_c)$ is the center of the ellipse, orientation β^j. For each finger in Fig. 2(b), we show its major axis along the finger and the minor crossing it.

Assume we are matching two finger contours: the query ϕ_M, and the template φ_N in the database. We use finger widths as finger features but they are measured during matching. The elliptic model of the template $\lambda_t = (\beta_t, T_t, L_t, W_t, C_t)$ is obtained during the enrollment stage. Its major axis $\overrightarrow{T_tC_t}$ is specially termed as the *principal axis* $\overrightarrow{OX}$ and a Cartesian coordinate system XOY is set up using its fingertip T_t as the origin O. This principal axis is fixed on the finger as well as its major axis $\overrightarrow{T_tC_t}$.

At the fingertip T_t of t, the contour is divided into two wings: the *up* wing and the *down* wing. Starting from T_t, along the direction of $\overrightarrow{T_tC_t}$, we partition the principal axis $\overrightarrow{OX}$ with an equal interval $\delta_x = x_{l+1} - x_l$ at a series of nodes x_l, $l \in [1, N_l]$. Passing x_l and parallel to $\overrightarrow{OY}$, straight line Y_l should normally have two crossover points with φ_N, at the up point (x_l, y_l^U) on the up wing and at the down point (x_l, y_l^D) on the down wing, where U and D in the superscripts refer to the up wing and the down wing respectively. At x_l, the Y-coordinate (y_l^U) of the up wing crossover point is defined as the signed up width, i.e., $w_l^U = y_l^U$. Similarly, that of the down wing is the signed down width $w_l^D = y_l^D$. The overall width feature of t at x_l is given by $w_l = |w_l^U - w_l^D|$. For the query finger q, the measurement of width features is similar except that q is superimposed on t in the same XOY system with every possible relative rotation and/or translation to t. We have up-widths $w_l^{U,q}$, down-widths $w_l^{D,q}$ and finger widths $w_l^q = |w_l^{U,q} - w_l^{D,q}|$ measured.

For a particular pair of rotation/translation α, the above widths are used to define the goodness of the alignment

$$\Lambda(t, q, \alpha) = \frac{1}{L_\alpha^q} \sqrt{\sum_{l=1}^{N_\alpha^q} (w_{l,\alpha}^t - w_{l,\alpha}^q)^2} \tag{3}$$

where $w_{l,\alpha}^t$ and $w_{l,\alpha}^q$ are the width features for t and q, respectively, L_α^q is the number of nodes, l is the node order along the principal axis for α and N_α^q is the number of common nodes of $w_{l,\alpha}^t$ and $w_{l,\alpha}^q$. Finally, the optimal alignment is found at $\breve{\alpha}$ such that $\Lambda(t, q, \breve{\alpha})$ is minimized. The *matching score* to measure the difference of the two hands, is defined as

$$D = \sum_{j=1}^{J} [\Lambda(t_j, q_j, \breve{\alpha}_j) L_{\breve{\alpha}_j}^{q,j}], \tag{4}$$

where $L_{\breve{\alpha}_j}^{q,j}$ is the number of nodes of the j-th finger of the query hand at the optimal alignment status.

3. EXPERIMENTAL RESULTS

Our experiments are carried out using the aforementioned peg-free system. To form a database, we have collected 540 hand images from 108 left hands with 5 samples each. These images are of 640×480 in size with 256 grey levels. The hand shapes in them are of different dimensions and shapes with various placements. The actual effective region for the hands' placement is about 400×350 in the center of each image. Of each hand, only four fingers excluding the thumb (thus $J = 4$) are used in the performance evaluation, and only the $\frac{5}{6}$ portion of the finger near its fingertip which is considered rigid is compared. For the false acceptance rate (or FAR), each sample of a hand is compared with every sample of other hands but not compared with those of the same hand. In our database, this generates 144450 $(5 \times 5 \times 108 \times 107/2)$ imposter-class matches. As for the false rejection rate (or FRR), each sample of a hand is compared with any other sample of the same hand but not compared with the same sample. This makes 1080 $(108 \times 5 \times 4/2)$ genuine-class matches in our database. As for the node interval, δ_x, it is fixed for all fingers but different for several experiments in question for ease of comparison. In Fig. 3(a) are shown the computed received operating characteristic curves for $\delta_x = 4, 8, 16, 32, 64$ pixels (corresponding to $k = 0, 1, 2, 3, 4$) respectively. As show in Fig. 3(b) the genuine-class distribution plotted with a solid line is separated well with the imposter-class (plotted with a dashed line).

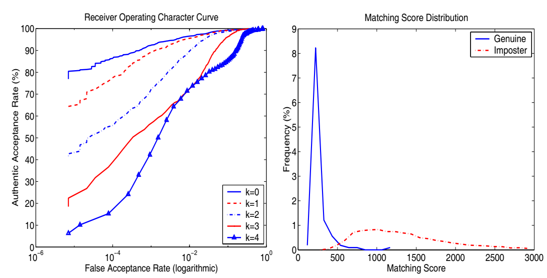

(a) (b)

Fig. 3. Performance of the hand geometry identification system: (a) ROC curves for hand identification with different node intervals, and (b) typical matching score histograms. The solid line stands for the scores of genuine-class matchings and the dashed line for the scores of imposter-class matchings.

Table 1. Identification performance at different resolutions: EER, FAR and AAR. Unit for δ_x and N_l is pixel.

	$k=0$	$k=1$	$k=2$	$k=3$	$k=4$
δ_x	4	8	16	32	64
N_l	45	23	12	6	4
EER(%)	2.41	2.60	3.33	6.60	12.65
FAR(%)	1.065	0.982	0.975	1.044	0.866
AAR(%)	96.64	95.51	89.53	72.81	71.50
FAR(%)	1.96	1.45	1.99	1.94	2.07
AAR(%)	97.48	97.01	94.30	78.13	77.20

Due to the lack of a common database, we are not able to make further fair comparisons with other existing works. To provide a reference for later researchers however, we try to keep the FAR near to 1% and 2%, (as in some references), in two experiments for each interval respectively. The major results are shown in Table 1.

4. CONCLUSION

We have addressed the problem of deformable hand shape recognition in hand-geometry biometric systems without any positioning aids in this work. Without the aids, the hand shapes have more deformation and we also lose the reference points to locate fingers for features extraction. The detection, localization and identification of fingers are no longer simple tasks in the traditional hand geometry verification systems. We decompose a hand contour into its individual rigid fingers and match them. This is similar to [3] but we use a different shape analysis method and adopt finger models to guide the optimal matching search. We achieve a good performance with an EER up to 2.41%. Further detail work regarding parameters selection will be published elsewhere[5].

5. REFERENCES

[1] Richard L. Zunkel, "Hand geometry based authentication," in *Biometrics: Personal Identification in Networked Society*, A. K. Jain, R. Bolle, and S. Pankanti, Eds. Kluwer Academic Publishers, 1998.

[2] Raul Sanchez-Reillo, Carmen Sanchez-Avila, and Ana Gonzalez-Marcos, "Biometric identification through hand geometry measurements," *IEEE Transaction on Pattern Analysis and Machine Intelligence*, vol. 22, no. 10, pp. 1168–1171, October 2000.

[3] A.K. Jain and Nicolae Duta, "Deformable matching of hand shapes for verification," in *Proceedings of International Conference on Image Processing*, Kobe, Japan, October 1999, vol. 2, pp. 857–861.

[4] Kar-Ann Toh, Wei Xiong, Wei-Yun Yau, and Xudong Jiang, "Combining fingerprint and hand-geometry verification decisions," in *Proceedings of 4th International Conference on Audio- and Video-Based Biometric Person Authentication*, Josef Kittler and Mark S. Nixon, Eds., Guildford, UK, June 2003, vol. AVBPA 2003, pp. 688–695, Springer-Verlag.

[5] Wei Xiong, Kar-Ann Toh, Wei-Yun Yau, and Xudong Jiang, "Model-guided deformable hand shape recognition without positioning aids," *Pattern Recognition*, 2004, Accepted.